Application of NEGF and NEGF+DFT to Magnetic Tunnel Junctions

Branislav K. Nikolić

Department of Physics & Astronomy, University of Delaware, Newark, DE 19716, U.S.A.

https://wiki.physics.udel.edu/phys824

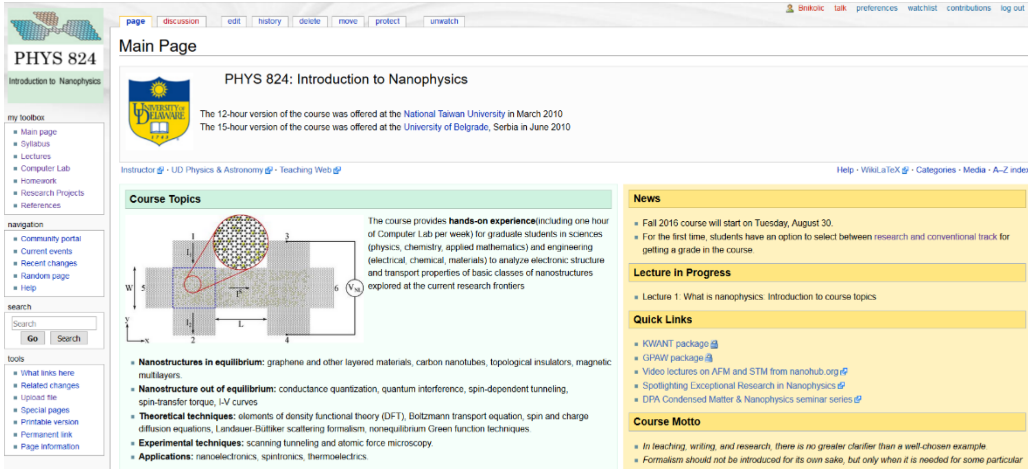

Magnetic Tunnel Junctions (MTJs): Fundamentals and Applications

Fundamentals

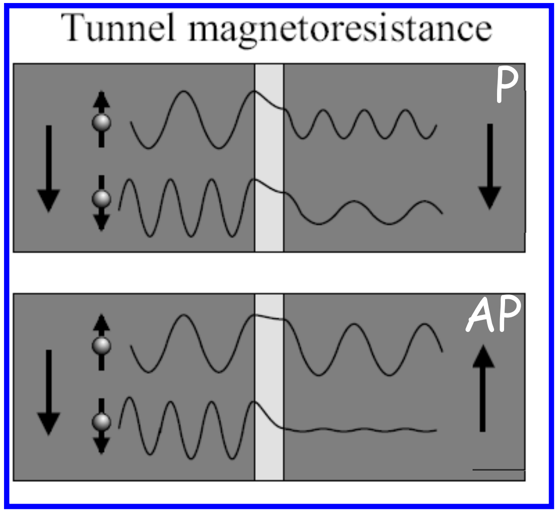

$$\mathrm{TMR}_{\mathrm{optimistic}} = \frac{R_{\mathrm{AP}} - R_{\mathrm{P}}}{R_{\mathrm{P}}}$$

$$\mathrm{TMR}_{\mathrm{pessimistic}} = \frac{R_{\mathrm{AP}} - R_{\mathrm{P}}}{R_{\mathrm{AP}}}$$

Applications

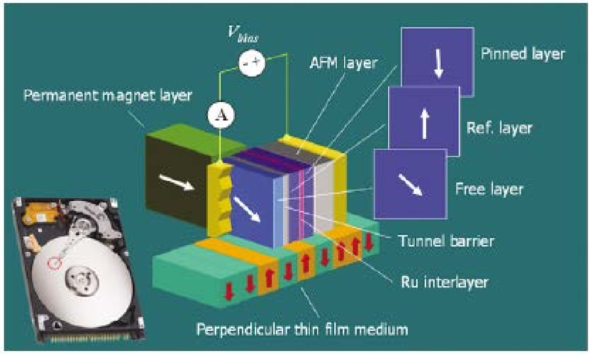

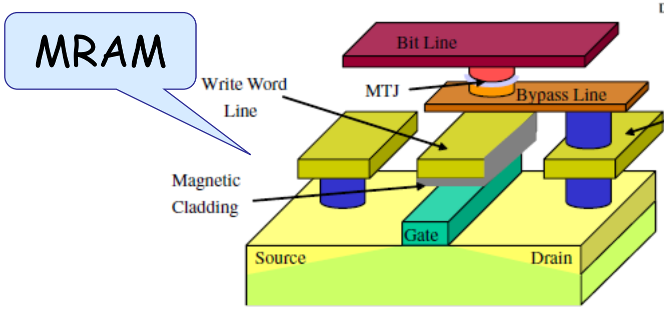

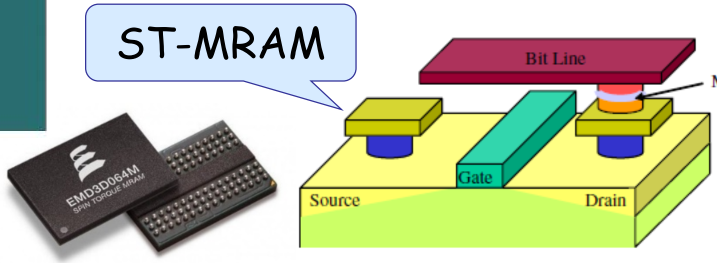

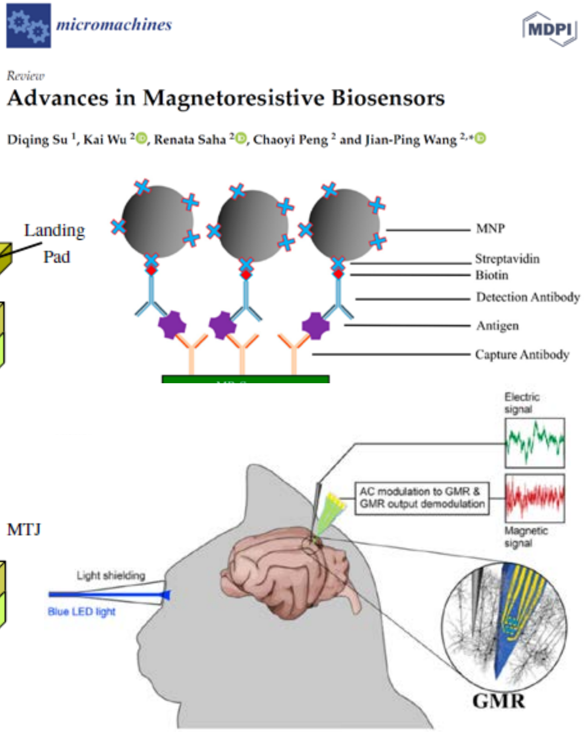

Fe/MgO/Fe MTJs as the Workhorse of Basic Research and Commercial Spintronics

NEGF+DFT predicts TMR ~ 1000% at small bias voltage

PHYSICAL REVIEW B, VOLUME 63, 054416

Spin-dependent tunneling conductance of Fe|MgO|Fe sandwiches

W. H. Butler, X.-G. Zhang, and T. C. Schulthess
Oak Ridge National Laboratory, Oak Ridge, Tennessee 37831-6114

J. M. MacLaren
Department of Physics, Tulane University, New Orleans, Louisiana 70018

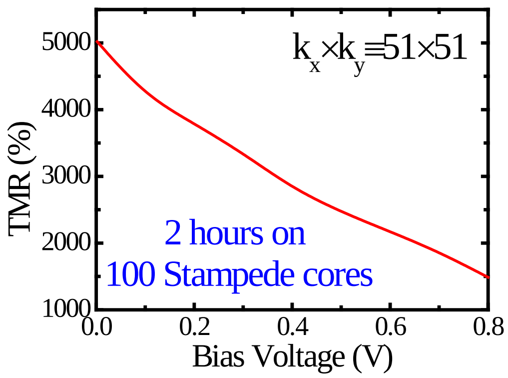

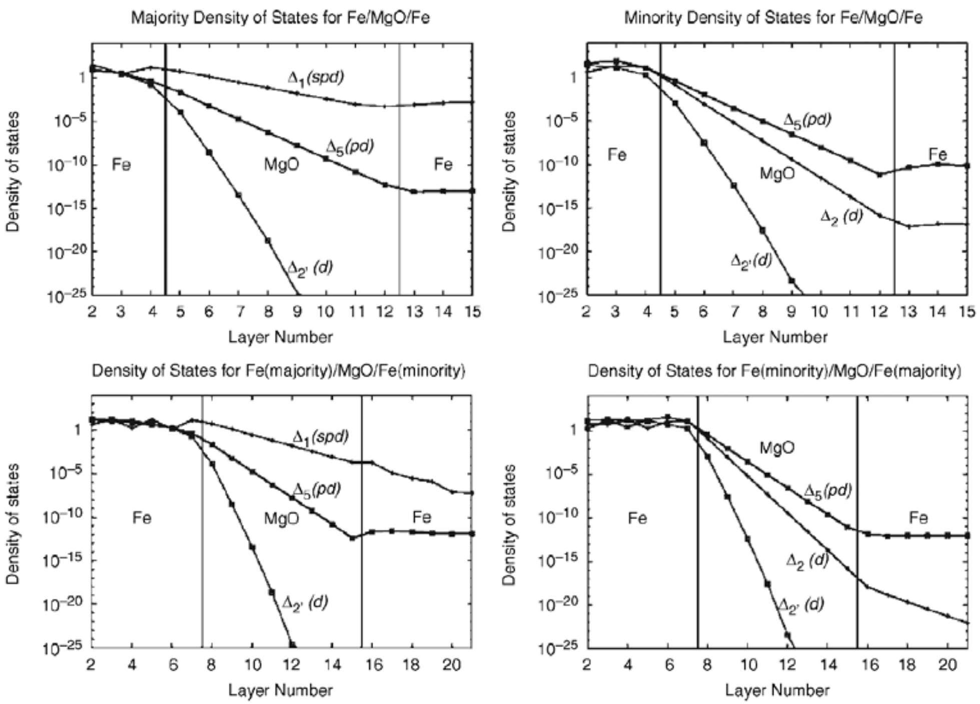

Experiment

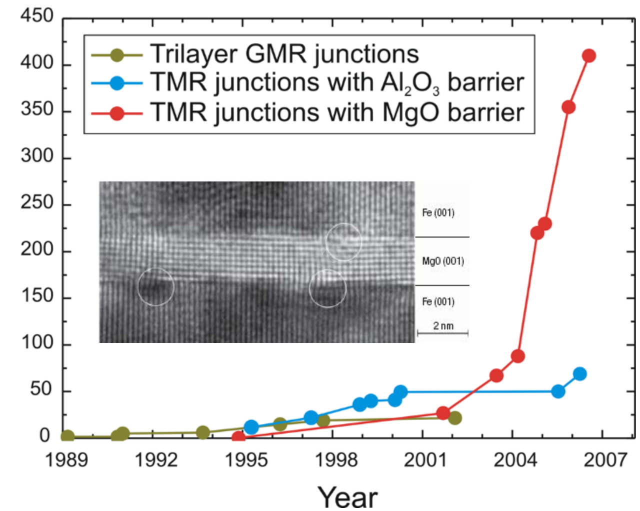

Nature Mater. **3**, 868 (2004)

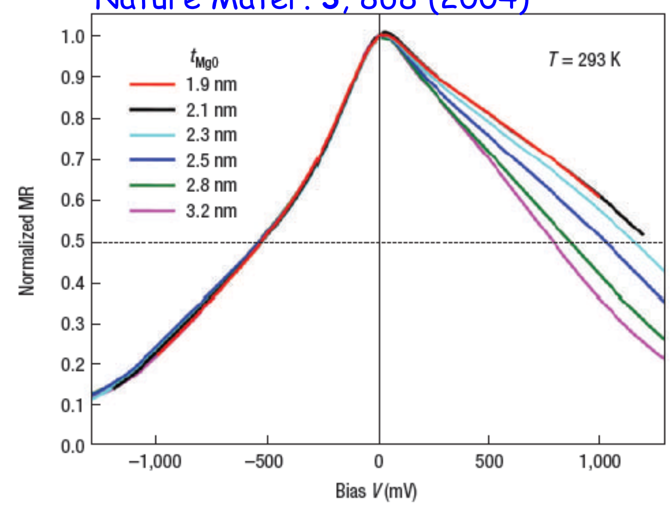

Switching by Magnetic Field vs. Current-Induced STT vs. VCMA

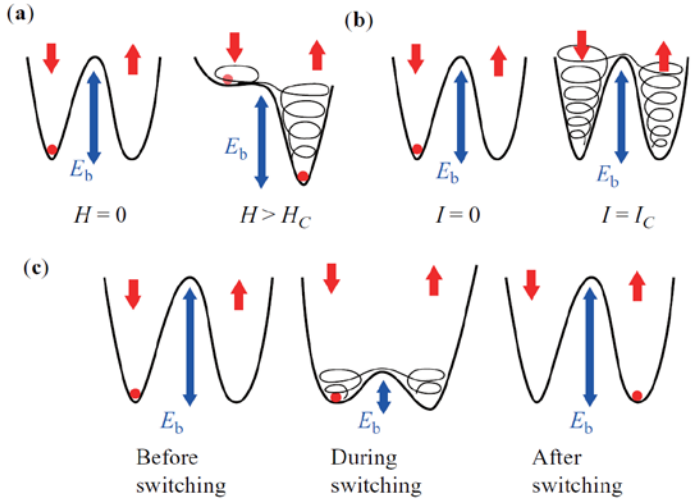

Schematic drawings of different switching methods: (a) field-induced switching; (b) STT switching; (c) voltage-controlled switching with a variable barrier height.

STT=Spin-Transfer Torque

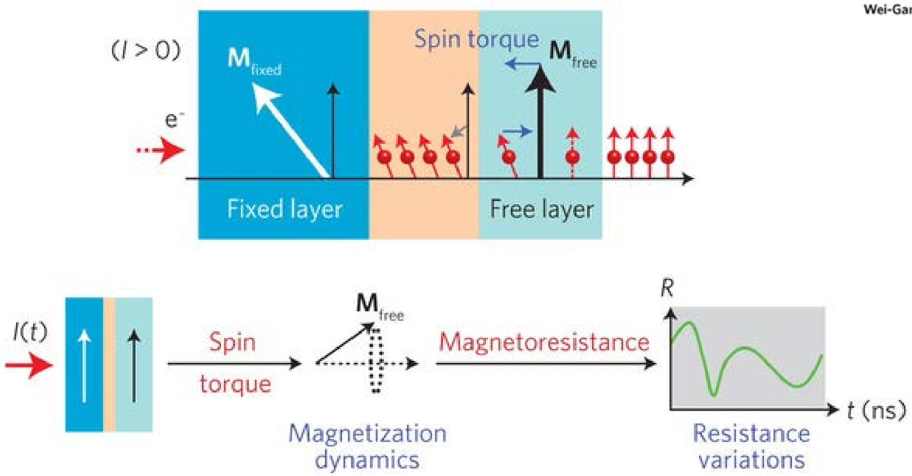

VCMA=Voltage-Controlled Magnetic Anisotropy

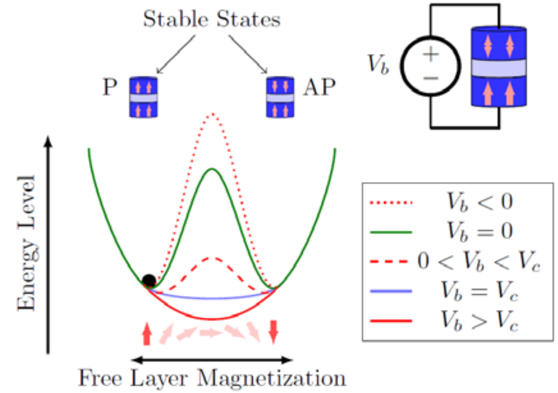

ARTICLES
PUBLISHED ONLINE: 13 NOVEMBER 2011 | DOI: 10.1038/NMAT3171
nature materials

Electric-field-assisted switching in magnetic tunnel junctions

Wei-Gang Wang*, Mingen Li, Stephen Hageman and C. L. Chien*

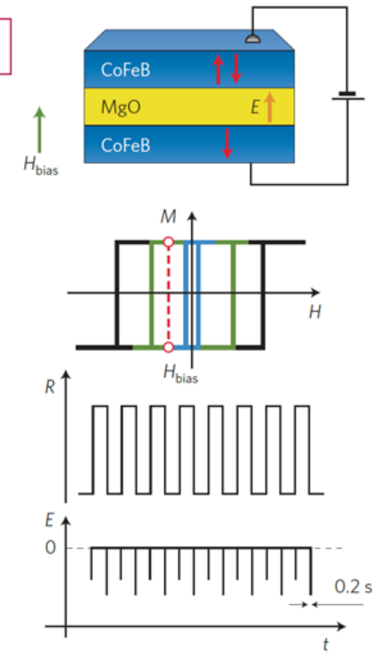

In-Plane vs. Perpendicular MTJs

❑Properties differ widely between the so-called "in-plane" and "perpendicular" MTJs → besides TMR ratio, most fundamental parameters for MTJs are thermal stability factor $\Delta = E_b/kBT$ (E_b is the energy barrier between the parallel and antiparallel states) and switching current I_c in spin-transfer torque, which characterize the performance in storing and writing information, respectively.

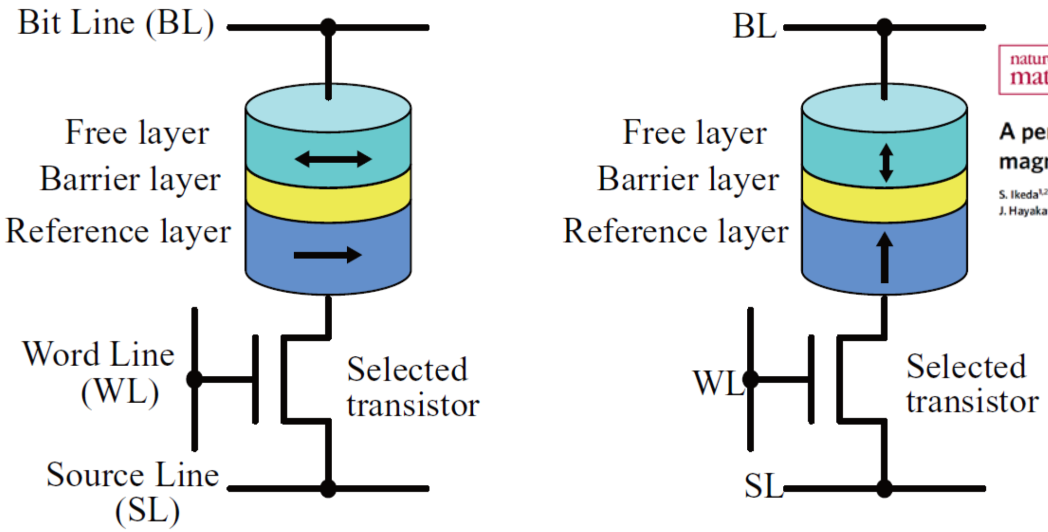

(**a**) In-plane MTJ (**b**) Perpendicular MTJ

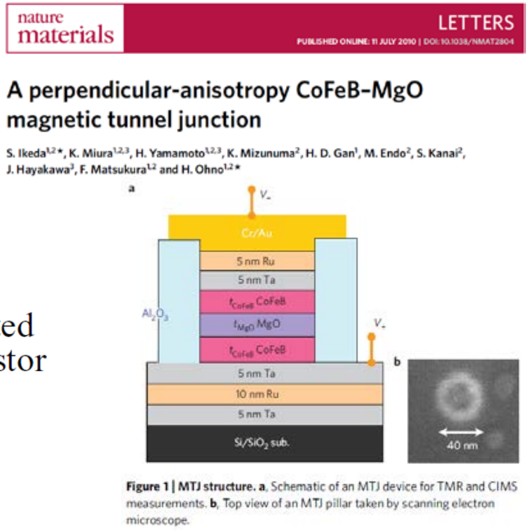
nature materials LETTERS
PUBLISHED ONLINE: 11 JULY 2010 | DOI: 10.1038/NMAT2804

A perpendicular-anisotropy CoFeB–MgO magnetic tunnel junction

S. Ikeda[1,2]*, K. Miura[1,2,3], H. Yamamoto[1,2,3], K. Mizunuma[2], H. D. Gan[1], M. Endo[2], S. Kanai[2], J. Hayakawa[3], F. Matsukura[1,2] and H. Ohno[1,2]*

Figure 1 | MTJ structure. a, Schematic of an MTJ device for TMR and CIMS measurements. **b**, Top view of an MTJ pillar taken by scanning electron microscope.

saturation magnetization; thickness of the free layer; aspect ratio (Width/Length of cross section); effective demagnetization field; Gilbert damping

$$\Delta_{\mathrm{IP}} = \frac{\pi^2 (M_S t)^2 W(\mathrm{AR}-1)}{k_B T}$$

$$I_{\mathrm{IP}}^{\mathrm{c}} = \frac{4ek_B T}{\hbar}\frac{\alpha}{\eta}\Delta_{\mathrm{IP}}\left(1+\frac{4\pi M_{\mathrm{eff}}}{2H_K}\right)$$

anisotropy field

$$\Delta_{\mathrm{PMA}} = \left(\sigma - 2\pi M_S^2 t\right)\frac{\pi \mathrm{AR} w^2}{4k_B T}$$

$$H_K = \frac{2\sigma}{M_S t} - 4\pi M_S$$

$$I_{\mathrm{PMA}}^{\mathrm{c}} = \frac{4ek_B T}{\hbar}\frac{\alpha}{\eta}\Delta_{\mathrm{PMA}}$$

Crash Course on NEGF for Steady-State Quantum Transport

❑Basic NEGF quantities:

density of available quantum states:

$$G^r_{\sigma\sigma'}(t,t') = -\frac{i}{\hbar}\Theta(t-t')\langle\{\hat{c}_{\mathbf{r}\sigma}(t),\hat{c}^\dagger_{\mathbf{r}'\sigma'}(t')\}\rangle$$

how are those states occupied:

$$G^<_{\sigma\sigma'}(t,t') = \frac{i}{\hbar}\langle\hat{c}^\dagger_{\mathbf{r}'\sigma'}(t')\hat{c}_{\mathbf{r}\sigma}(t)\rangle$$

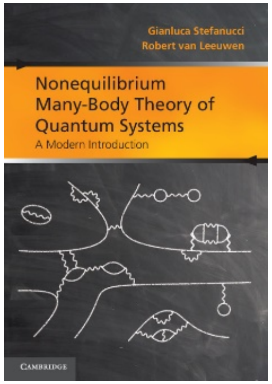

❑NEGFs for steady-state transport:

$$G^r(t,t') \rightarrow G^r(t-t') \xrightarrow{\text{FT}} G^r(E)$$

$$G^<(t,t') \rightarrow G^<(t-t') \xrightarrow{\text{FT}} G^<(E)$$

$$\boldsymbol{\rho}_{\text{eq}} = -\frac{1}{\pi}\int_{-\infty}^{+\infty} dE\, \text{Im}\, \mathbf{G}^r(E) f(E-E_F)$$

$$\boldsymbol{\rho}_{\text{neq}} = \frac{1}{2\pi i}\int_{-\infty}^{+\infty} dE\, \mathbf{G}^<(E)$$

❑NEGF (quantum) vs. Boltzmann (semiclassical) nonequilibrium statistical mechanics:

$$G^r(E) = [E - H - \Sigma^r_{\text{leads}} - \Sigma^r_{\text{int}}]^{-1}$$

$$G^<(E) = G^r(E)[\Sigma^<_{\text{leads}}(E) + \Sigma^<_{\text{int}}(E)]G^a(E)$$

$$\mathbf{v}\cdot\nabla f + \mathbf{F}\cdot\nabla_{\mathbf{k}} f = I_{\text{coll}}[f]$$

$$\mathbf{j} = 2_s e \int \frac{d^3\mathbf{k}}{(2\pi)^3}\mathbf{v}(\mathbf{k}) f(\mathbf{k})$$

❑NEGF-based current expression for two-terminal nanostructures:

$$I_\alpha = \frac{e}{h}\int dE\, \text{Tr}\left[\boldsymbol{\Sigma}^<_\alpha(E,V_b)\mathbf{G}^>(E) - \boldsymbol{\Sigma}^>_\alpha(E,V_b)\mathbf{G}^<(E,V_b)\right]$$

Meir-Wingreen formula

$$I_R(V_b) = -I_L(V_b) = \frac{e}{h}\int dE\, \text{Tr}\left[\boldsymbol{\Gamma}_R(E,V_b)\mathbf{G}^r(E,V_b)\boldsymbol{\Gamma}_L(E,V_b)\mathbf{G}^a(E,V_b)\right][f_L(E) - f_R(E)]$$

Landauer-Büttiker formula for the limit of quantum-coherent transport where inelastic (e-e, e-ph, e-m) processes are absent

TMR of 1D Tight-Binding Model of FM/I/FM MTJ: Exact Analytical Solution via NEGF

Without spin

NM — 1 (I) — NM

$\Sigma_1 = -\frac{i}{2}[\gamma_1]$, $\quad H = [\varepsilon]$, $\quad \Sigma_2 = -\frac{i}{2}[\gamma_2]$

$\Gamma_1 = [\gamma_1]$, $\quad \Gamma_2 = [\gamma_2]$

With spin

up / dn: FM — 1 (I) — FM

$$\Sigma_1 = -\frac{i}{2}\begin{bmatrix}\gamma_{1u} & 0 \\ 0 & \gamma_{1d}\end{bmatrix}, \quad H = \begin{bmatrix}\varepsilon & 0 \\ 0 & \varepsilon\end{bmatrix}, \quad \Sigma_2 = -\frac{i}{2}\begin{bmatrix}\gamma_{2u} & 0 \\ 0 & \gamma_{2d}\end{bmatrix}$$

$$\Gamma_1 = \begin{bmatrix}\gamma_{1u} & 0 \\ 0 & \gamma_{1d}\end{bmatrix}, \quad \Gamma_2 = \begin{bmatrix}\gamma_{2u} & 0 \\ 0 & \gamma_{2d}\end{bmatrix}$$

assuming: $E_F - \varepsilon \gg k_B T, \alpha, \beta$

$$\left.\begin{aligned} G_{\rm P} &= \frac{e^2}{h} T_{\rm P}(E_F) \approx \frac{\alpha^2+\beta^2}{(E_F-\varepsilon)^2} \\ G_{\rm AP} &= \frac{e^2}{h} T_{\rm AP}(E_F) \approx \frac{2\alpha\beta}{(E_F-\varepsilon)^2} \end{aligned}\right\} \Rightarrow \left\{\begin{aligned} &\mathrm{TMR} = \frac{G_{\rm P}-G_{\rm AP}}{G_{\rm AP}} = \frac{2P^2}{1-P^2} \\ &P = \frac{\alpha-\beta}{\alpha+\beta} \end{aligned}\right.$$

spin-polarization of electrons in each of two identical FM leads

$\Uparrow$

P:

$$\left.\begin{aligned}\gamma_{1u} = \gamma_{2u} \equiv \alpha \\ \gamma_{1d} = \gamma_{2d} \equiv \beta\end{aligned}\right\} \Rightarrow \mathbf{\Gamma}_1 = \mathbf{\Gamma}_2 = \begin{pmatrix}\alpha & 0 \\ 0 & \beta\end{pmatrix}; T_{\rm P}(E) = \mathrm{Tr}\left[\mathbf{\Gamma}_2 \mathbf{G}^r \mathbf{\Gamma}_1 \mathbf{G}^a\right] = \mathrm{Tr}\left[\begin{pmatrix}\alpha & 0 \\ 0 & \beta\end{pmatrix}\begin{pmatrix}E-\varepsilon+\frac{i}{2}2\alpha & 0 \\ 0 & E-\varepsilon+\frac{i}{2}2\beta\end{pmatrix}^{-1}\begin{pmatrix}\alpha & 0 \\ 0 & \beta\end{pmatrix}\left[\mathbf{G}^r\right]^\dagger\right] = \frac{\alpha^2}{(E-\varepsilon)^2+\alpha^2} + \frac{\beta^2}{(E-\varepsilon)^2+\beta^2}$$

AP:

$$\left.\begin{aligned}\gamma_{1u} = \gamma_{2d} \equiv \alpha \\ \gamma_{1d} = \gamma_{2u} \equiv \beta\end{aligned}\right\} \Rightarrow \mathbf{\Gamma}_1 = \begin{pmatrix}\alpha & 0 \\ 0 & \beta\end{pmatrix}; \mathbf{\Gamma}_2 = \begin{pmatrix}\beta & 0 \\ 0 & \alpha\end{pmatrix}; T_{\rm AP}(E) = \mathrm{Tr}\left[\mathbf{\Gamma}_2 \mathbf{G}^r \mathbf{\Gamma}_1 \mathbf{G}^a\right] = \mathrm{Tr}\left[\begin{pmatrix}\beta & 0 \\ 0 & \alpha\end{pmatrix}\begin{pmatrix}E-\varepsilon+\frac{i}{2}(\alpha+\beta) & 0 \\ 0 & E-\varepsilon+\frac{i}{2}(\alpha+\beta)\end{pmatrix}^{-1}\begin{pmatrix}\alpha & 0 \\ 0 & \beta\end{pmatrix}\left[\mathbf{G}^r\right]^\dagger\right] = \frac{2\alpha\beta}{(E-\varepsilon)^2+\left(\frac{\alpha+\beta}{2}\right)^2}$$

- Compare with heuristic "Julier formula" (1975):

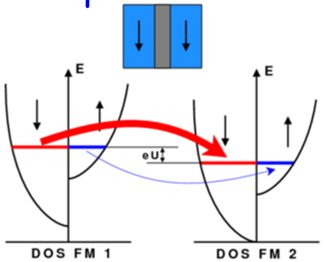

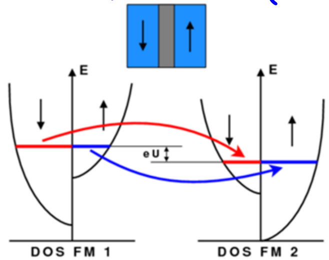

$$\mathrm{TMR} = \frac{2P_1P_2}{1-P_1P_2}$$

$$P_{1,2} = \frac{D^{\uparrow}_{1,2}(E_F) - D^{\downarrow}_{1,2}(E_F)}{D^{\uparrow}_{1,2}(E_F) + D^{\downarrow}_{1,2}(E_F)}$$

naively, spin-polarization is determined by spin-resolved DOS in the bulk of FM leads

Crash Course on NEGF+DFT for Steady-State First-Principles Quantum Transport

❑Primary physical reason for NEGF+DFT self-consistent loop, which computes charge redistribution due to **current flow at finite bias voltage**, is to ensure gauge invariance of I-V characteristics

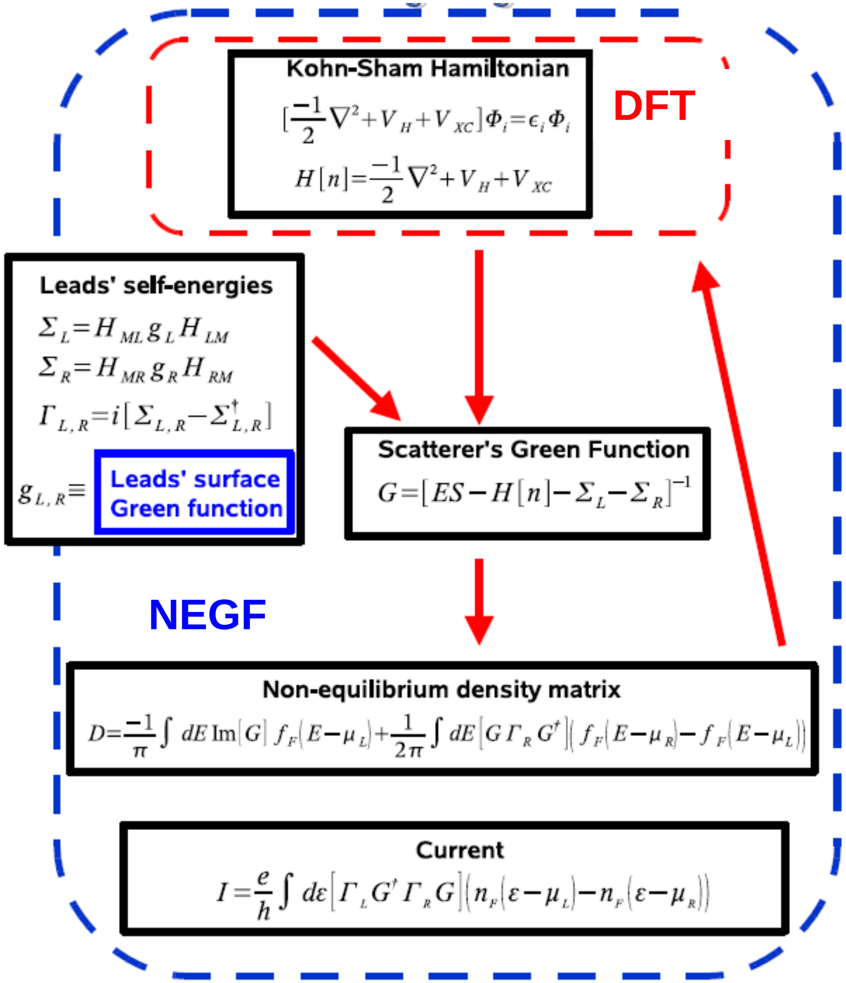

EUROPHYSICS LETTERS

Europhys. Lett., **35** (7), pp. 523-528 (1996)

Gauge-invariant nonlinear electric transport in mesoscopic conductors

T. CHRISTEN[1] and M. BÜTTIKER[1,2]

Smeagol
Non-equilibrium Electronic Transport

Trans siesta

GPAW!

QuantumATK

PHYSICAL REVIEW B **79**, 205430 (2009)

***I-V* curve signatures of nonequilibrium-driven band gap collapse in magnetically ordered zigzag graphene nanoribbon two-terminal devices**

Denis A. Areshkin and Branislav K. Nikolić

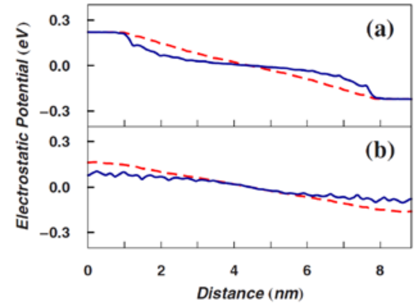

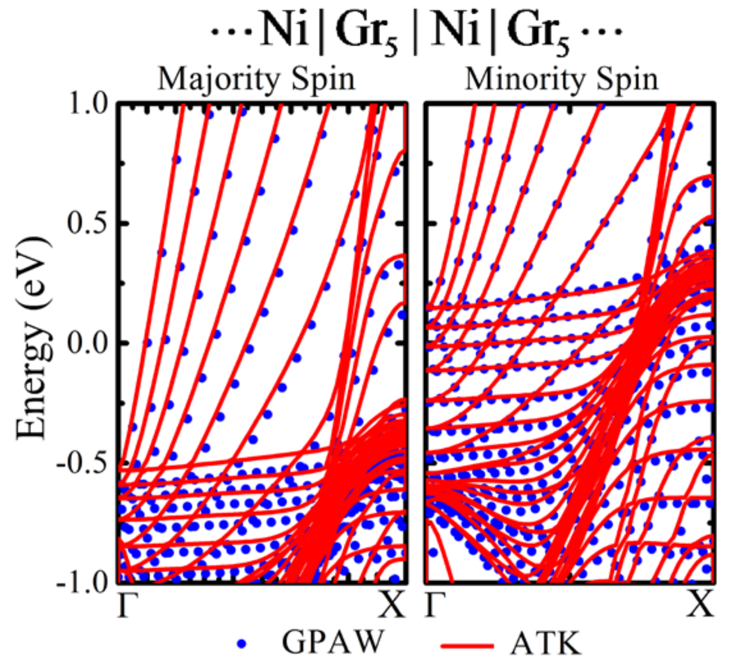

Ni: double-zeta polarized, C: single-zeta polarized

Challenges for NEGF+DFT in Application to Modeling of Realistic Nanodevices

- Large systems (in excess of 10,000 atoms)

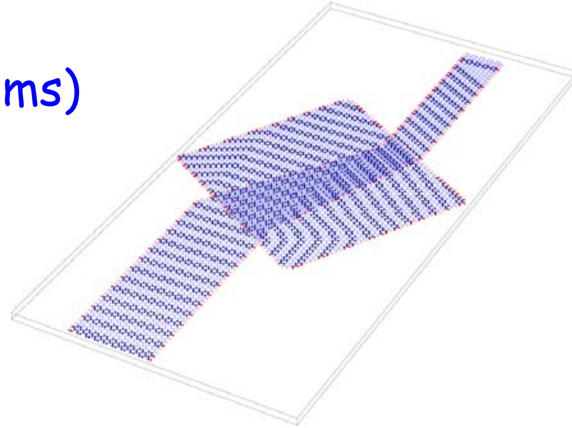

- The electrostatic potential may be determined by a dynamical environment (for instance a solvent)

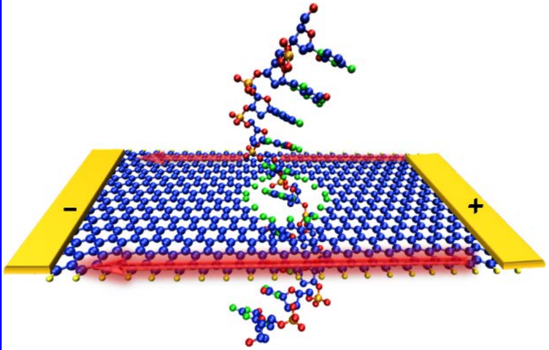

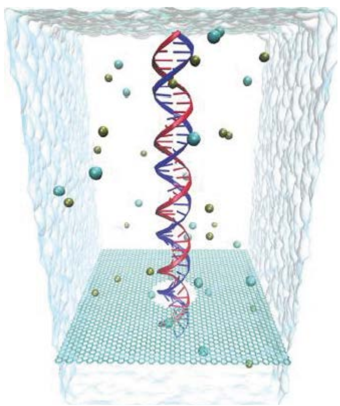

- Many-body effects

$$\hat{H} = \hat{H}_{\mathrm{e}}^0 + \hat{H}_{\mathrm{ph}}^0 + \hat{H}_{\mathrm{e\text{-}ph}} = \sum_{i,j} H_{ij}^0 \hat{c}_i^\dagger \hat{c}_j + \sum_{i,j} \hbar\omega_\lambda \hat{a}_\lambda^\dagger \hat{a}_\lambda + \sum_{\lambda,i,j} M_{ij}^\lambda \hat{c}_i^\dagger \hat{c}_j (\hat{a}_\lambda^\dagger + \hat{a}_\lambda)$$

empirical models or DFT (GPAW) computed

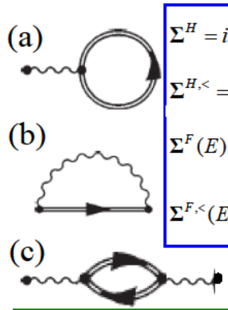

$$\mathbf{\Sigma}^H = i\sum_\lambda \frac{2}{\omega_\lambda}\int \frac{dE'}{2\pi}\mathbf{M}^\lambda \mathrm{Tr}\left[\mathbf{G}_0^<(E')\mathbf{M}^\lambda\right]$$

$$\mathbf{\Sigma}^{H,<} = 0$$

$$\mathbf{\Sigma}^F(E) = i\sum_\lambda \int \frac{dE'}{2\pi}\mathbf{M}^\lambda \begin{bmatrix} \mathbf{D}_0(E-E')\mathbf{G}_0^<(E') + \mathbf{D}_0(E-E')\mathbf{G}_0(E') \\ +\mathbf{D}_0^<(E-E')\mathbf{G}_0(E') \end{bmatrix} \mathbf{M}^\lambda$$

$$\mathbf{\Sigma}^{F,<}(E) = i\sum_\lambda \int \frac{dE'}{2\pi}\mathbf{M}^\lambda \mathbf{D}_0(E-E')\mathbf{G}_0^<(E')\mathbf{M}^\lambda$$

electron self-energies in SCBA

$$\mathbf{\Pi}(\omega) = -i\sum_\lambda \int \frac{dE'}{2\pi}\mathbf{M}^\lambda \begin{bmatrix} \mathbf{G}_0(E')\mathbf{G}_0^<(E'-\omega) + \\ \mathbf{G}_0^<(E)\mathbf{G}_0^\dagger(E'-\omega) \end{bmatrix} \mathbf{M}^\lambda$$

$$\mathbf{\Pi}^<(\omega) = -i\sum_\lambda \int \frac{dE'}{2\pi}\mathbf{M}^\lambda \mathbf{G}_0^<(E)\mathbf{G}_0^>(E'-\omega)\mathbf{M}^\lambda$$

phonon self-energies in SCBA

second-order diagrams

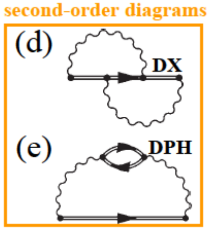

Ni/Vertical-Gr_n/Ni as MTJ with Perfect Spin Filtering

PRL **99**, 176602 (2007) PHYSICAL REVIEW LETTERS week ending 26 OCTOBER 2007

Graphite and Graphene as Perfect Spin Filters

V. M. Karpan,[1] G. Giovannetti,[1,2] P. A. Khomyakov,[1] M. Talanana,[1] A. A. Starikov,[1] M. Zwierzycki,[3] J. van den Brink,[2,4] G. Brocks,[1] and P. J. Kelly[1]

Fermi surface projected to the direction of transport

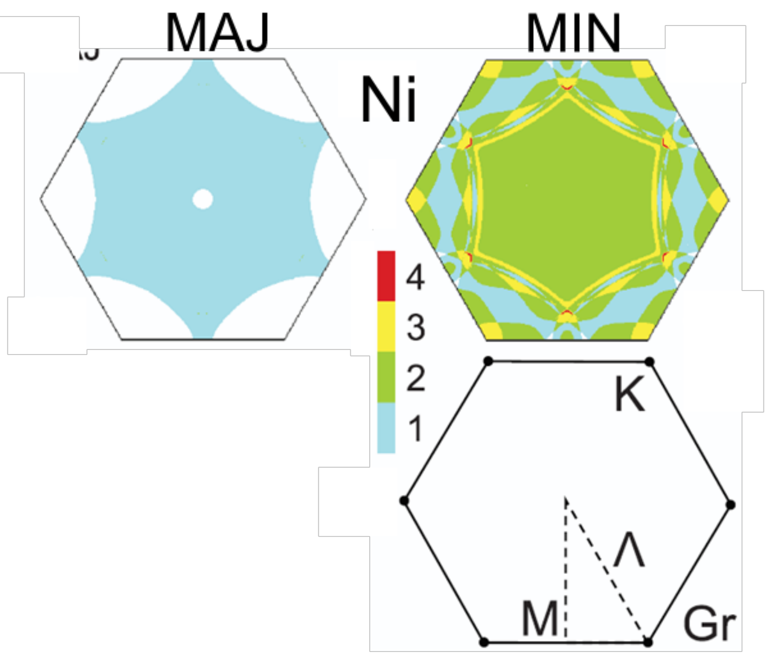

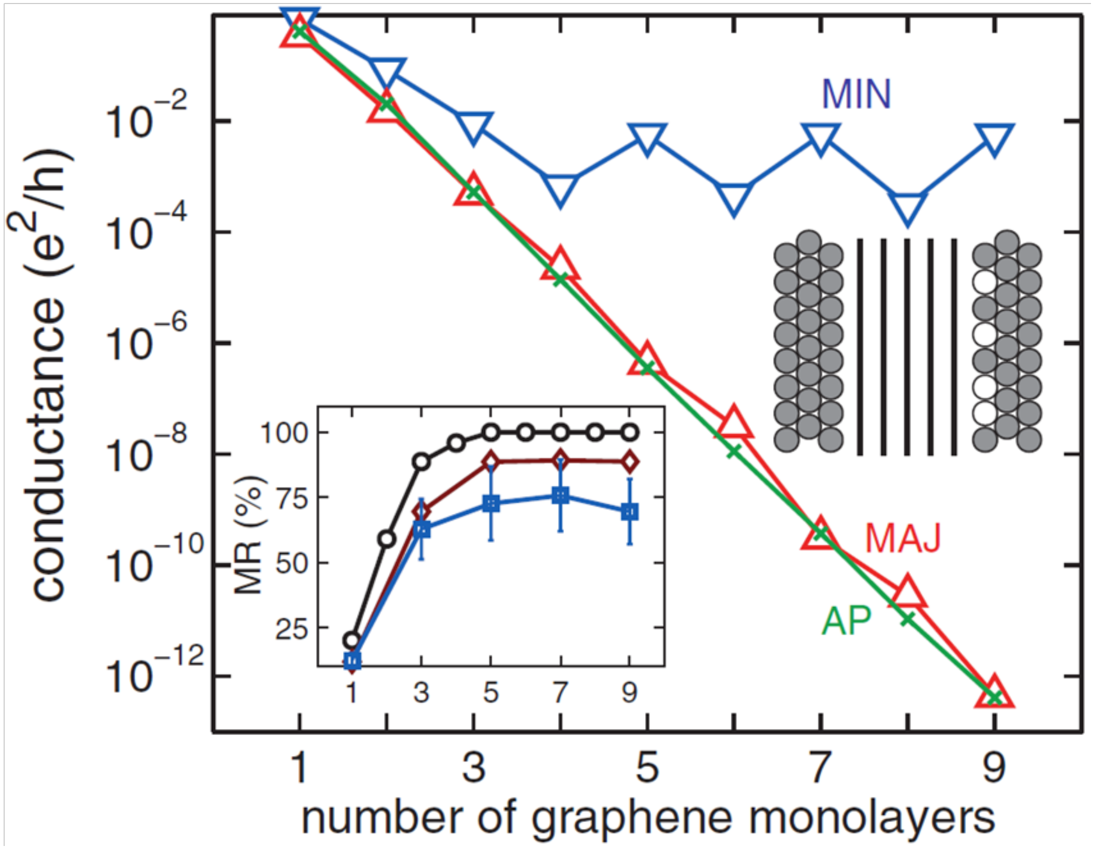

Important of Small Mismatch Between Lattices of Electrode and Barrier Materials

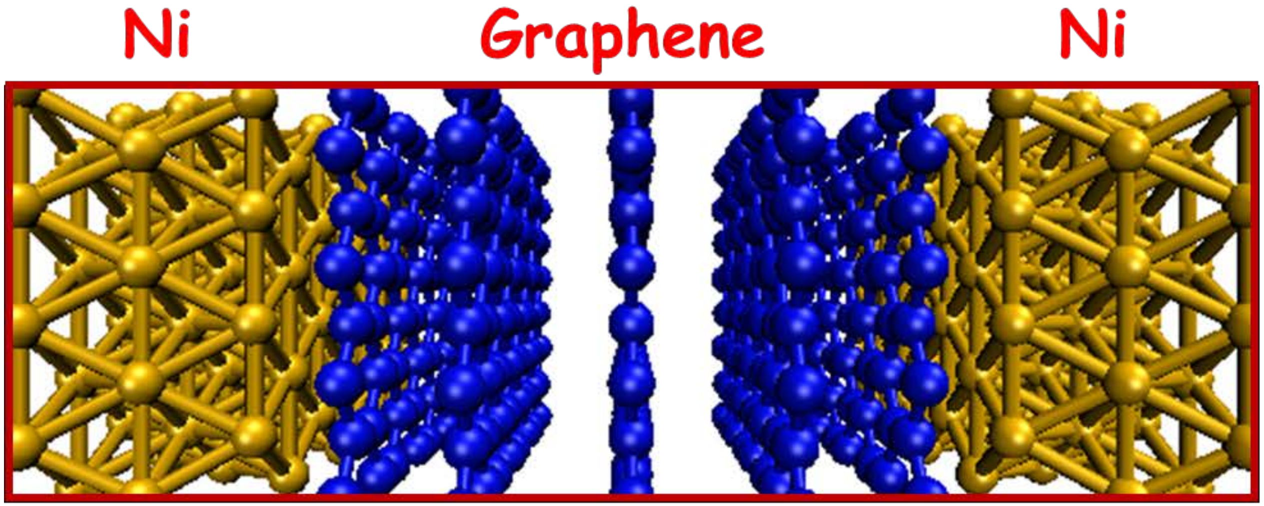

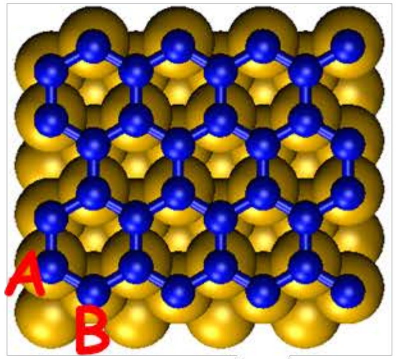

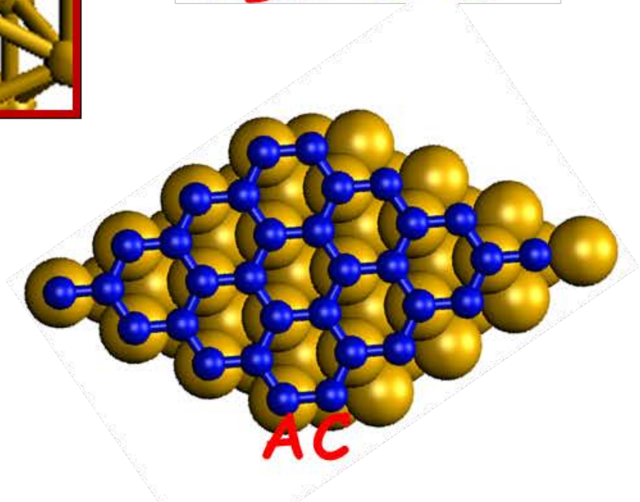

Q: Why Ni as electrode?

- Only 1.3% in-plane lattice mismatch
- Majority spin states of Ni are absent around the K-point where graphene states reside

Magnetoresistance of Ni/Gr_n/Ni at Zero or at Finite Bias Voltage

TMR$_{pesimistic}$ ~ 100% @ V_{bias} = 0 and for sufficiently thick (n=5) vertical graphene barrier

PHYSICAL REVIEW B 85, 184426 (2012)

Magnetoresistance and negative differential resistance in Ni/graphene/Ni vertical heterostructures driven by finite bias voltage: A first-principles study

Kamal K. Saha,[1] Anders Blom,[2] Kristian S. Thygesen,[3] and Branislav K. Nikolić[1,*]

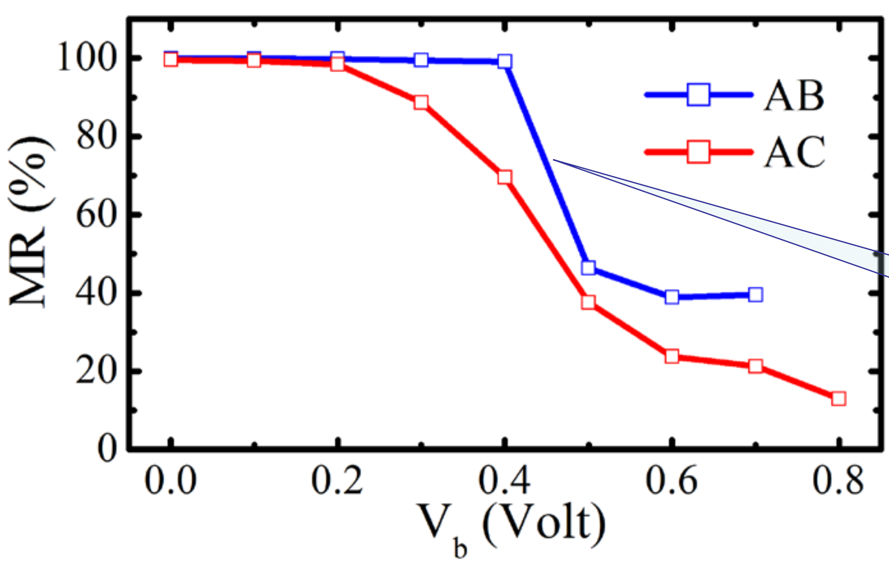

MR ~ 100% @ V_{bias} ≤ 0.4 V

Bias-Voltage-Dependent Transmission Function and Negative Differential Resistance (NDR) in Ni/Gr_n/Ni

PHYSICAL REVIEW B **85**, 184426 (2012)

Magnetoresistance and negative differential resistance in Ni/graphene/Ni vertical heterostructures driven by finite bias voltage: A first-principles study

Kamal K. Saha,[1] Anders Blom,[2] Kristian S. Thygesen,[3] and Branislav K. Nikolić[1,*]

NDR means that current decreases with increasing V_b

Parallel

Antiparallel

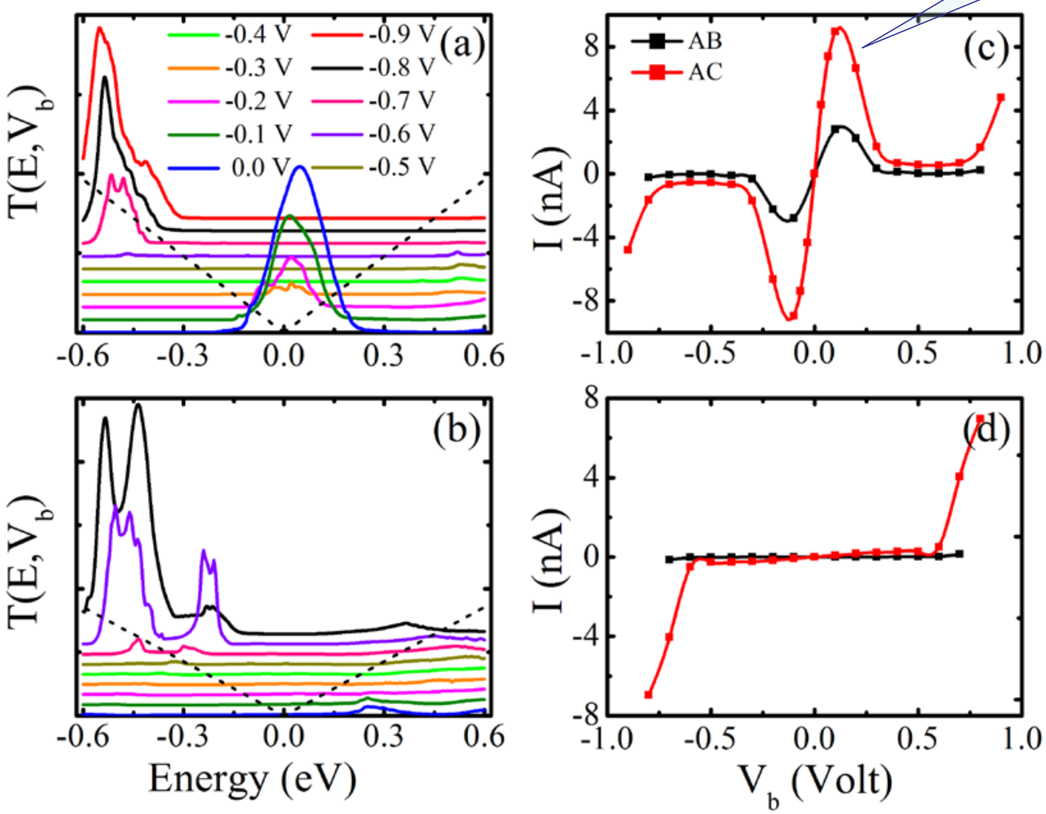

Can one apply ~1 V bias voltage across Gr_n?

APL **98**, 133112 (2011)

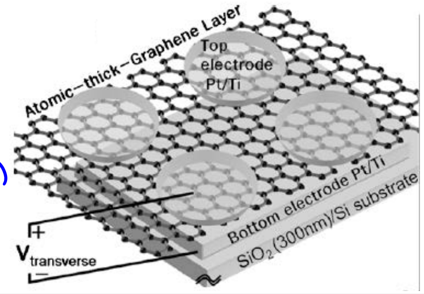

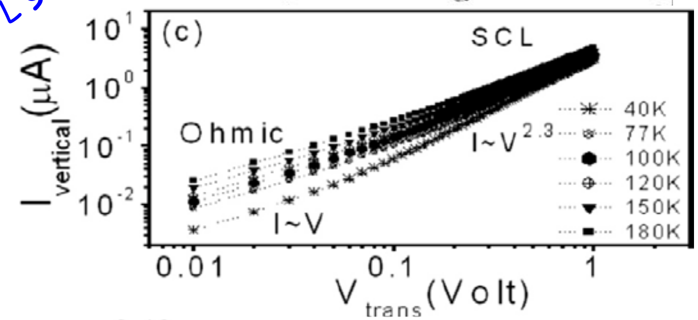

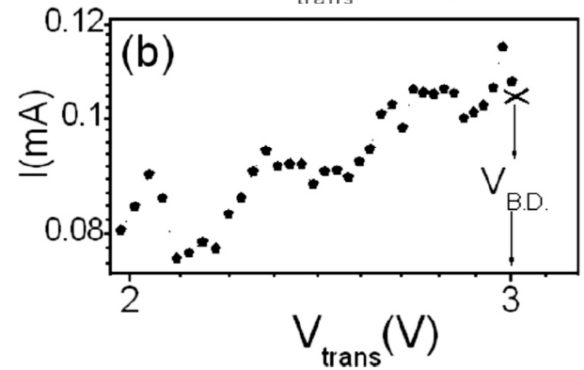

Voltage-Dependent Local Density of States as a Tool to Understand Origin of NDR

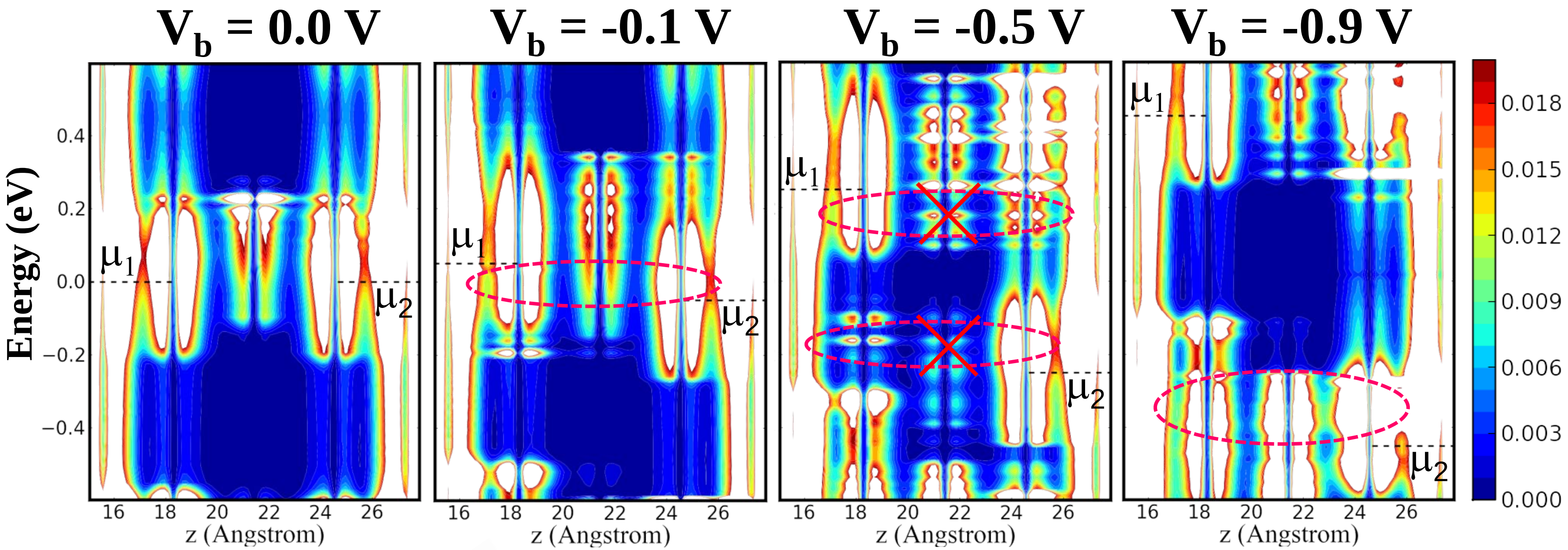

PHYSICAL REVIEW B **85**, 184426 (2012)

Magnetoresistance and negative differential resistance in Ni/graphene/Ni vertical heterostructures driven by finite bias voltage: A first-principles study

Kamal K. Saha,[1] Anders Blom,[2] Kristian S. Thygesen,[3] and Branislav K. Nikolić[1,*]

$$\text{LDOS} = -\frac{1}{\pi}\,\text{Im}\,G^r(E,z,z;V_b)$$

Progress in Experimental Realization of Ferromagnet/Gr_n/Ferromagnet Junctions

J. Phys. D: Appl. Phys. 50 (2017) 203002 (16pp) https

Topical Review

2D-MTJs: introducing 2D materials in magnetic tunnel junctions

Maëlis Piquemal-Banci, Regina Galceran, Marie-Blandine Martin, Florian Godel, Abdelmadjid Anane, Frederic Petroff, Bruno Dlubak and Pierre Seneor

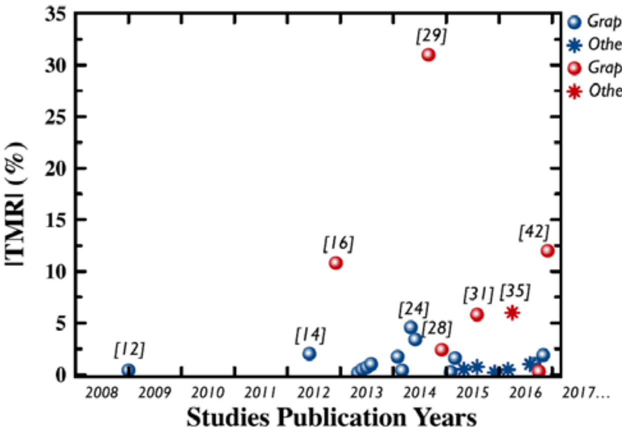

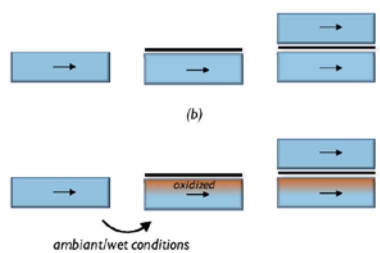

Figure 7. (a) In the case of a direct CVD on top of the bottom ferromagnet, the graphene layer is grown on a metallic surface. Its strong resistance to diffusion, in particular regarding oxygen, prevents oxidation. The resulting MTJs thus possess two preserved ferromagnetic interfaces. (b) In the case of a simple exfoliation or transfer process, the bottom ferromagnetic electrode is exposed to air and to wet chemistry. The graphene layer thus traps an already oxidized interface. This leads to the fabrication of MTJs with a degraded interface that strongly quenches the performance of the device.

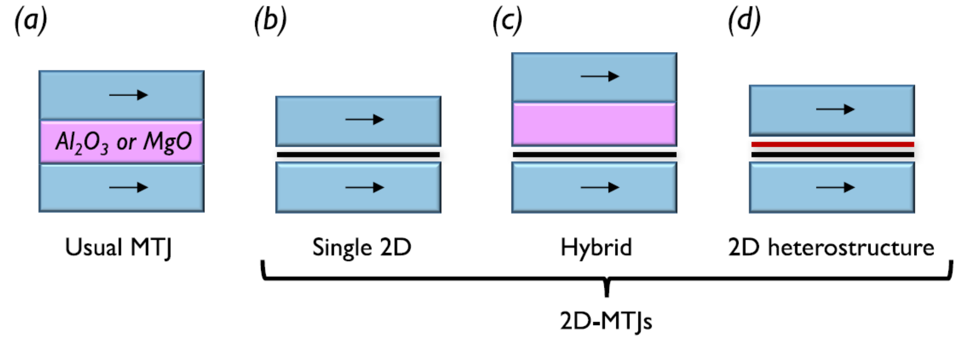

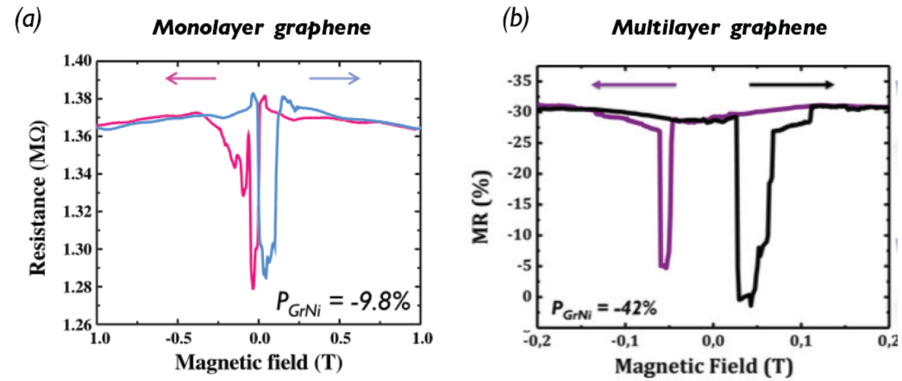

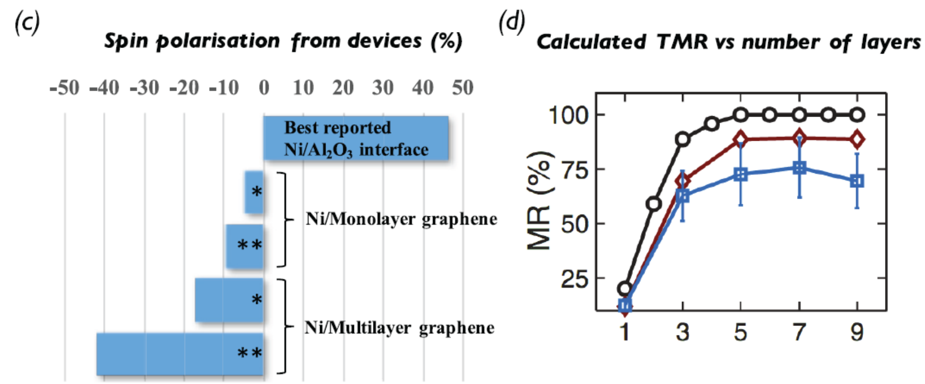

Materials Science & Engineering of Graphene on Ni(111)

New J. Phys. **12**, 125004 (2010)
New J. Phys. **13**, 025001 (2011)

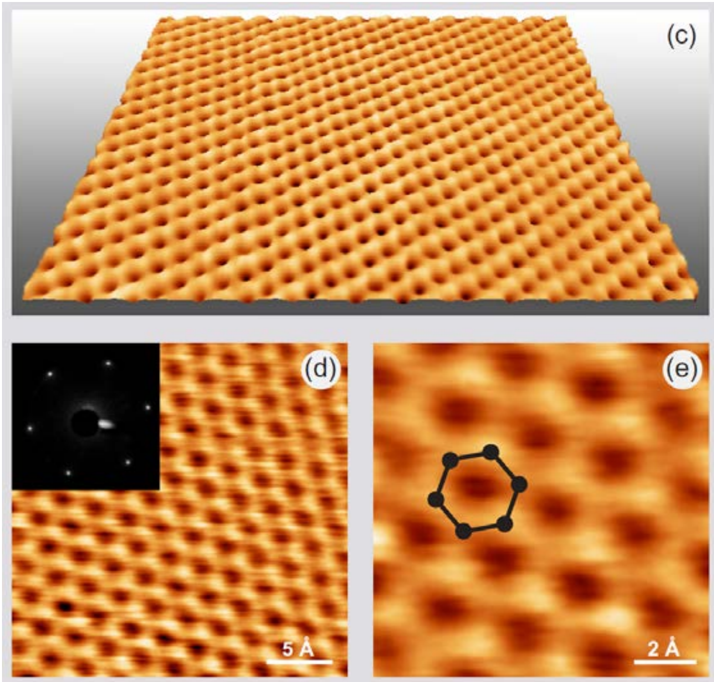

- graphene grows on Ni but not the other way around
- at temperatures between 480 C and 650 C, graphene grows on a pure Ni(111) surface in the absence of a carbide
- below 480 C, graphene growth competes with the formation of a surface Ni_2C carbide
- destabilization of the surface carbide by the addition of Cu to the surface layer facilitates the nucleation and growth of graphene at temperatures below 480 C

Challenges for DFT calculations: Standard LDA and GGA XC functionals do not work

PHYSICAL REVIEW B **84**, 201401(R) (2011)

Graphene on Ni(111): Strong interaction and weak adsorption

F. Mittendorfer,[1,*] A. Garhofer,[1] J. Redinger,[1] J. Klimeš,[2] J. Harl,[3] and G. Kresse[3]

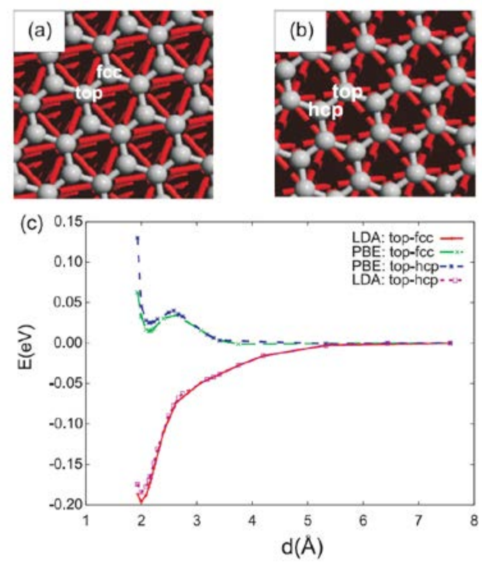

FIG. 1. (Color online) Graphene adsorption on Ni(111) in a top-fcc (a) and top-hcp (b) configuration. (c) DFT adsorption energies vs distance *d* calculated with the LDA (red and pink lines) and the PBE exchange-correlation functional (green and blue lines).

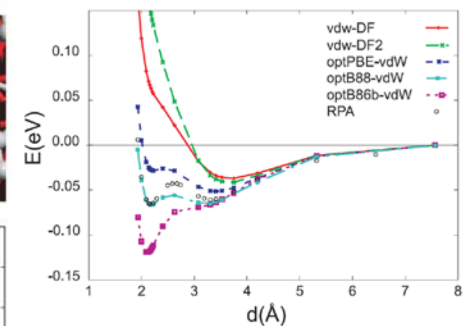

FIG. 4. (Color online) Adsorption of graphene (top fcc) on Ni(111) using the vdW DFT as a function of the exchange-correlation functional.

Many-Body Inelastic Effects in Quantum Transport in MTJs: Electron-Magnon and Electron-Phonon Scattering

Experiment:

PHYSICAL REVIEW B **77**, 014440 (2008)

Evidence for strong magnon contribution to the TMR temperature dependence in MgO based tunnel junctions

V. Drewello,* J. Schmalhorst, A. Thomas, and G. Reiss

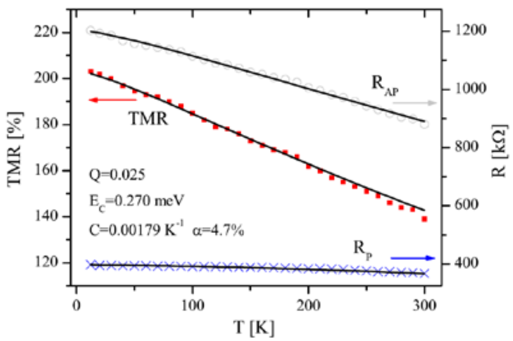

FIG. 1. (Color online) Resulting fit for the TMR temperature dependence of our MgO MTJ using the magnon excitation model and thermal smearing.

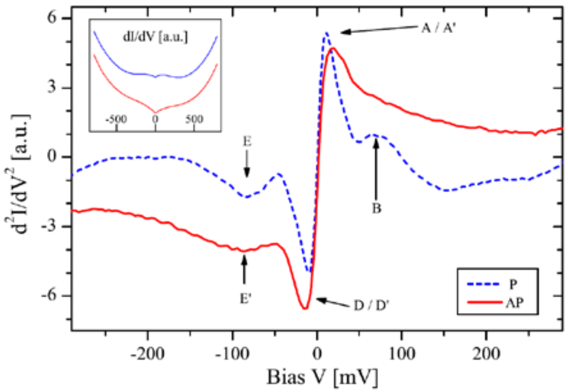

FIG. 2. (Color online) IET spectra of a MgO MTJ in a parallel (dashed line) and antiparallel (solid line) state at 12 K. Typical magnon (A, D) and phonon (B, E) peaks can be identified in parallel and antiparallel (e.g., A′) configuration.

Theory & Computation:

PHYSICAL REVIEW B **90**, 045115 (2014)

Signatures of electron-magnon interaction in charge and spin currents through magnetic tunnel junctions: A nonequilibrium many-body perturbation theory approach

Farzad Mahfouzi* and Branislav K. Nikolić†

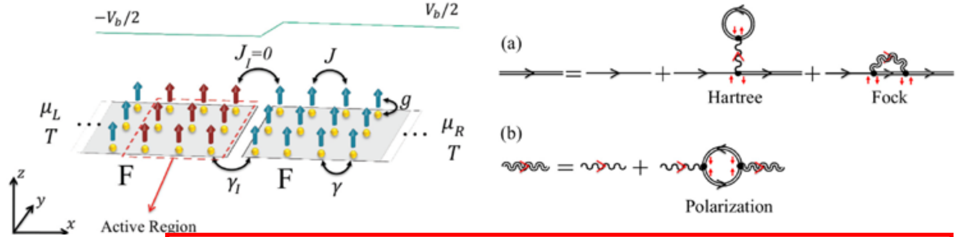

$$I_\alpha = I_\alpha^{\rm el} + I_\alpha^{\rm inel}$$

$$I_\alpha^{\rm el} = \frac{e}{h}\sum_\beta \int dE\, {\rm Tr}(\mathbf{\Gamma}_\alpha \mathbf{G}^r \mathbf{\Gamma}_\beta \mathbf{G}^a)(f_\beta - f_\alpha),$$

$$I_\alpha^{\rm inel} = \frac{e}{h}\int dE\, {\rm Tr}(\mathbf{G}^r \mathbf{\Sigma}^{>,F} \mathbf{G}^a \mathbf{\Sigma}_\alpha^{<} - \mathbf{G}^r \mathbf{\Sigma}^{<,F} \mathbf{G}^a \mathbf{\Sigma}_\alpha^{>})$$